Colloid Polym Sci (2008) 286:673–681
DOI 10.1007/s00396-007-1811-9

ORIGINAL CONTRIBUTION

# Miscibility studies of PVC/Aramid blends

**Saima Shabbir · Sonia Zulfiqar · Muhammad Ishaq · Muhammad Ilyas Sarwar**

Received: 18 October 2007 / Revised: 17 November 2007 / Accepted: 25 November 2007 / Published online: 4 January 2008


**Abstract** Blends containing PVC and aramid (Ar) matrices were probed for their miscibility. In this respect, Ar chains were synthesized by aromatic diamine and diacid chloride in amide solvent. The Ar thus synthesized was characterized through Fourier transform infrared (FTIR) spectroscopy and molecular weight determination. Blend system Ar/PVC was investigated over a range of Ar/PVC ratios. Their mechanical profiles in terms of maximum stress, maximum strain, toughness, and initial moduli have been explored. Thermal properties and morphology of the blends were estimated using thermogravimetric analysis (TGA), differential scanning calorimetry (DSC), and scanning electron microscopy (SEM). A good correlation was observed between thermal, mechanical, and morphological properties of the blends. The presence of hydrogen bonding among polymers was evaluated through FTIR spectroscopy, which is believed to be responsible for the blend miscibility. Optimal thermal and mechanical profiles were depicted by the blend containing 40-wt% PVC in the Ar matrix.

**Keywords** Morphology · Mechanical properties · PVC · Aramid

## Introduction

Polyvinyl chloride (PVC) plays an important role in the plastic industry and is one of the most versatile thermoplastics, but it must be combined with a number of additives before processing. The addition of plasticizers to a PVC formulation decreases many mechanical properties such as hardness, tensile strength, modulus, etc. of the PVC product; however, low temperature flexibility, elongation and the ease of processing are all improved [1]. Therefore, it is imperative to augment thermal stability and processability without deteriorating mechanical properties. PVC is known for its efficiency to form miscible systems with several other low and high molecular weight substances acting as plasticizers. In both cases, specific interaction through hydrogen bonding between the blend components is suggested to be the basis of miscibility [2–4]. Both melt-mixed [5] and solution cast [6] blends have been explored to display a single glass transition temperature ($T_g$) lying between that of blend constituents. Polymer blending has been reported to have a great impact on the thermal stability [7–12]; several researchers have shown that compatibility between two components in a binary blend is one of the decisive factors that determine the thermal stability of polymer blends [13–16]. Varughese [7] reported that the blending of epoxidized natural rubber (ENR) with polyvinyl chloride reduced the rate of HCl elimination in the first degradation step of PVC. The blending of a polymer with other polymers has stabilizing and destabilizing effects. In miscible polymer blends, there are often specific interactions between groups or polymer segments that lead to a decrease of the Gibbs free energy of mixing [17]. Hydrogen bonding has great potential for controlling macromolecular assembly and organization [18–20]. Hence, hydrogen bonding has been used for improvement of the polymer–polymer compatibility and the formation of macromolecular aggregations [18–23]. PVC has a serious drawback in that it degrades under processing and end-use conditions, accompanied with discoloration and deteriora-

S. Shabbir · S. Zulfiqar · M. Ishaq · M. I. Sarwar (✉)
Department of Chemistry, Quaid-i-Azam University,
Islamabad 45320, Pakistan
e-mail: ilyassarwar@hotmail.com

tion of its mechanical properties. The thermal degradation of PVC during processing is well known to be caused by the liberation of hydrogen chloride at the labile sites of the PVC molecular chain [24–27]. To improve processability and thermal stability during molding and practical use, various stabilizers, lubricants, and impact modifiers are added to the PVC.

The aim of the present study is to prepare polymer blends by combination of tuning the balance of interactions and macromolecular composition. For this purpose, an aramid (Ar) matrix has been synthesized by solution polymerization of 4,4′-oxydianiline (ODA) and isophthaloyl chloride (IPC) in *N*,*N*-dimethylacetamide (DMAc) solvent. The synthesized aromatic polyamide served as a constituent in the subsequent PVC/Ar blends. Blend compositions have been varied over a range of Ar and PVC ratios to monitor the morphology, thermal, and mechanical profiles of the system. Improvement of thermal, mechanical, and morphological behaviors have been perused because of hydrogen bonding operating between the hydrogen atom of PVC and carbonyl group of polyamide, thus rendering the miscibility of two matrices.

## Experimental section

### Materials and methods

Polyvinyl chloride (PVC) with molecular weight 100,000 was supplied by BDH and used after drying under vacuum at 40°C for 24 h. *N*,*N*-dimethylacetamide (DMAc) anhydrous was obtained by the courtesy of Aldrich. The monomers used for the preparation of Ar, 4,4′-oxydianiline (ODA), and isophthaloyl chloride (IPC), were procured from Fluka and used as received.

### Synthesis of Ar matrix

Ar was synthesized by the solution polymerization of aromatic diamine and diacid chloride under anhydrous conditions. 4,4′-oxydianiline (ODA) was dissolved in DMAc as a solvent under an inert atmosphere. After complete mixing, stoichiometric amount of IPC was added giving highly exothermic reaction, hence, to avoid any side reactions, the contents were cooled to 0°C. Solvent employed for low temperature poly-condensation reaction leading to Ar was DMAc. For the solution polymerization of aromatic polyamide, however, no organic solvent is sufficiently powerful to keep the polymer in solution as the molecular weight of the polymer builds up. So, amide solvent such as DMAc with a small amount of HCl is considered a better solvent than amid alone. The DMAc and HCl (produced during the polymerization reaction of diamine and diacid chloride) furnish the desired salt–solvent combination with increased solubility for Ar. Moreover, HCl salt concentration increases as the polycondensation proceeds, thereby, enhancing the solvating power of the solvent as the molecular weight of the polymer builds up. Although reaction between diamine and diacid chloride is extremely fast, however, further 24 h were given to the reaction for its completion. The reaction mixture was highly viscous and golden yellow in color. The chemical reaction leading to the formation of aromatic polyamide is presented in Scheme 1.

### Blend preparation

Different proportions of PVC were blended with Ar matrix giving Ar/PVC blends. Blend samples were obtained by solution mixing using DMAc as solvent. Component polymers, weighed to desired composition, were dissolved in the solvent and stirred until the solution became clear. Subsequently, the solvent was evaporated on petri dishes at

**Scheme 1** Synthesis of aromatic polyamide (Ar)

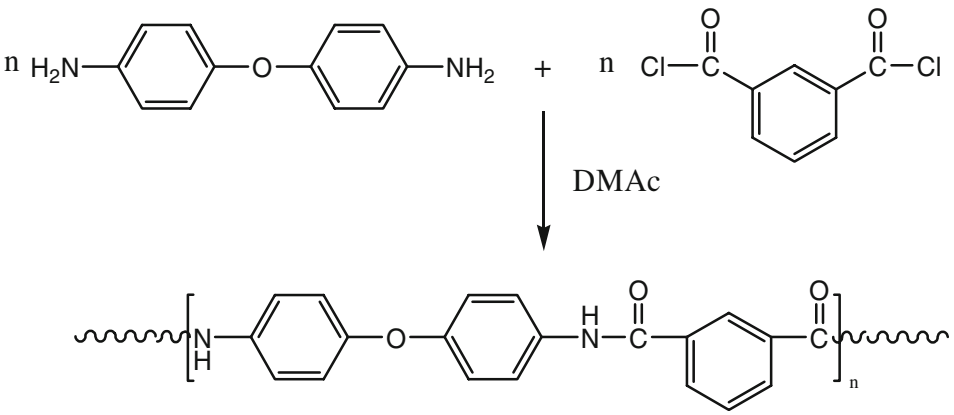

60°C. Films were washed repeatedly with distilled water for the removal of HCl produced during polymerization reaction. Before characterization, films were dried at 80°C under vacuum for 72 h.

### Characterization

The Fourier transform infrared (FTIR) study was carried out on thin films by using Excalibur Series FT-IR Spectrometer, model no. FTSW 300 MX manufactured by BIO-RAD. One hundred scans at a resolution of 4 $cm^{-1}$ were signal averaged. Stress–strain response of the blend samples with (ca 14×5.4–8.0×0.25–0.62 mm) dimensions was monitored according to Deutsches Institut Rir Normung (DIN) procedure 53455 having crosshead speed of 5 mm/min using Testometric Universal Testing Machine M350/550. Standard procedures and formulae were applied to calculate various tensile properties including stress, strain, initial modulus, and toughness. Tensile behavior of the samples was determined by plotting these stress–strain values using software origin 5.0 [28]. For phase morphological studies, samples were cryogenically fractured in liquid nitrogen, and the morphology of the blends was investigated with LEO GEMINI 1530 scanning electron microscope (SEM). Thermal stability of the blends was determined using METTLER TOLEDO TGA/SDTA $851^e$ thermo gravimetric analyzer by using 1–5 mg of the sample in $Al_2O_3$ crucible heated from 25 to 900°C at a heating rate of 10°C/min under nitrogen atmosphere with a gas flow rate of 30 ml/min. In order to obtain glass transition temperature differential scanning calorimetry (DSC) was performed using a METTLER TOLEDO DSC $822^e$ differential scanning calorimeter, samples of 5–10 mg were encapsulated in aluminum pans and heated at a rate of 10°C/min under nitrogen atmosphere. To determine the weight average molecular weight $<M_w>$ of aromatic polyamide, static laser light scattering (LLS) technique was employed using an ALV-SP81 laser Goniometer, which consists of a 20-mW uniphase He/Ne-Laser ($\lambda_o$=633 nm) and an ALV-5000 digital correlator; Langen, Hessen (Germany).

## Results and discussion

Polymeric blend compositions using Ar and PVC prepared by solution blending technique were pinkish in color. The mechanical properties were measured at 25°C, and the average value was obtained from five to seven different measurements in each case has been reported. For the sake of better interpretation of results, the blend compositions were divided into two systems.

### Laser light scattering

Light scattering is the absolute method for the determination of molecular weights. Static laser light scattering (LLS) measurement was performed on aromatic polyamide to determine the weight average molecular weight $<M_w>$. The sample was kept at constant temperature (20°C) during the experiment. Solution for light scattering prepared in DMSO was preliminarily filtered using a 0.45 μm Millipore Teflon syringe filter, to eliminate the impurities and dust. Then, the light intensity scattered from the clarified solution at different scattering angles was measured. For static LLS, the instrument was calibrated with toluene to ensure that there was no angular dependence of the scattered light from toluene. The details of the LLS instrumentation and theory can be found elsewhere [29, 30]. The weight average molecular weight $<M_w>$ of the synthesized Ar was determined to be $9.18\times10^4$ g/mol (± 3%) which is indicative of fairly high molecular weight aromatic polyamide. The Ar thus obtained was employed in the preparation of various blend compositions.

### FTIR spectroscopy

The structure of synthesized Ar was characterized by using FTIR spectroscopic analysis. The peaks above 3,260 $cm^{-1}$ show the N–H stretching, and those at 3,125 and 3,056 $cm^{-1}$ correspond to the aromatic C–H stretching vibrations, while peaks in the region of 1,600 to 1,635 $cm^{-1}$ were attributed to the clusters of C=O groups. The broadening of the peak indicated the C=O in different environments, i.e., amide C=O both free and hydrogen bonded. The group of closely related peaks at 1,500 $cm^{-1}$ were ascribed to aromatic C=C stretching, and the sharp peak at 1,318 $cm^{-1}$ represented –C–O–C– linkage (Fig. 1).

In the FTIR spectra of Ar/PVC blends of various concentrations, the major peaks observed were in the range of 1,600–1,690 $cm^{-1}$ for carbonyl stretching and 1,500 $cm^{-1}$ for aromatic C=C stretching in Ar chains. Peaks at 1,231–1,321 $cm^{-1}$ may be credited for C–H (H–C–Cl) in PVC chains. The peaks in region of 600 to 700 $cm^{-1}$ indicate the C–Cl stretching. Blend spectra clearly reveal that by increasing the amount of PVC in Ar /PVC blends, the height of the absorption peaks for C=O stretching (1,600–1,690 $cm^{-1}$) was decreased and broadened. This flattening and decrease in the height of absorption peak approved the hydrogen bonding between the C=O of amide and hydrogen of PVC (Fig. 2). In the FTIR spectrum of pure Ar, there was no peak for aliphatic C–H stretching. Similarly, the FTIR spectrum of the PVC had no aromatic C–H stretching, while in the blend spectra, both aromatic and aliphatic C–H peaks were present, demonstrating that PVC chains were incorporated

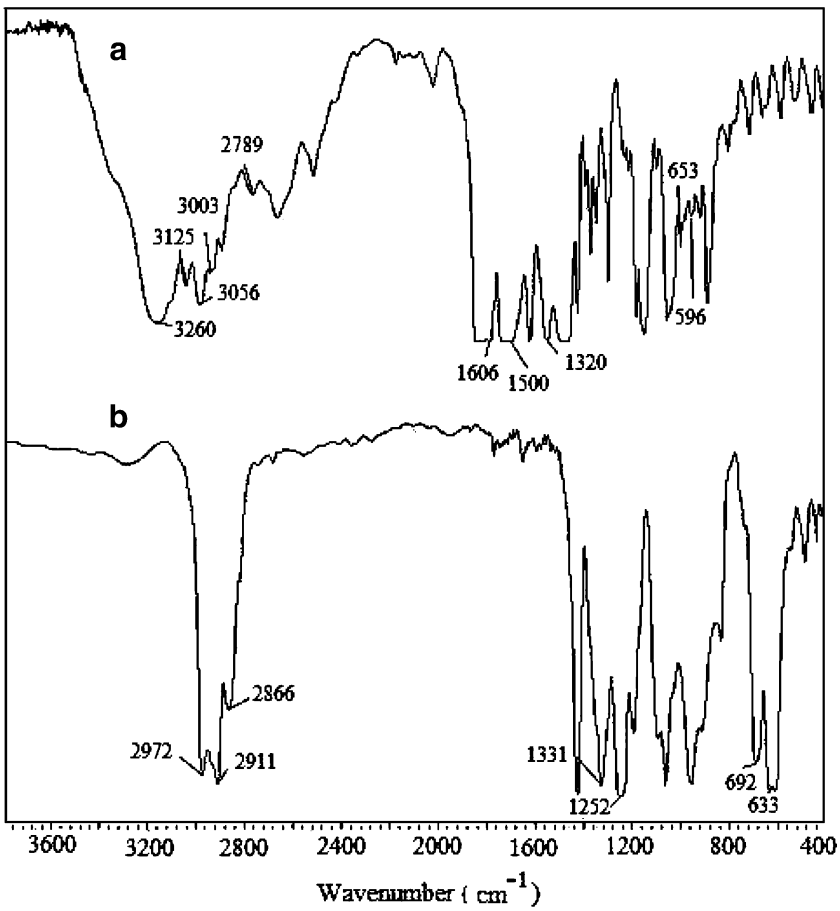


**Fig. 1** FTIR spectra of **a** Aramid and **b** PVC

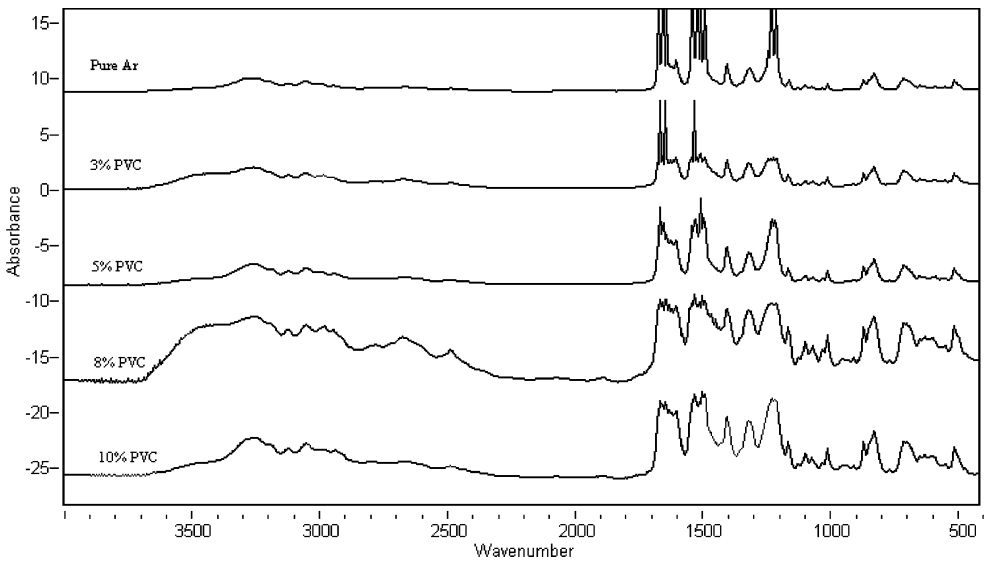


**Fig. 2** FTIR spectra of Ar/PVC blends with varying PVC compositions

**Table 1** Mechanical data of Ar-PVC blends

| Percent PVC | Maximum stress (MPa) ±0.03 | Maximum strain ±0.03 | Modulus (MPa) ±0.02 | Toughness (MPa) ±0.50 |
|---|---|---|---|---|
| 0 | 70.37 | 1.00 | 2288.97 | 62.00 |
| 10 | 31.23 | 2.64 | 709.47 | 64.19 |
| 20 | 33.88 | 2.34 | 798.54 | 58.66 |
| 30 | 39.81 | 2.34 | 1145.52 | 84.21 |
| 40 | 96.61 | 1.73 | 2299.06 | 159.53 |
| 50 | 29.12 | 3.33 | 327.89 | 74.28 |
| 100 | 10.20 | 2.52 | 531.80 | 22.52 |

into the chains of Ar. Furthermore, in the blend spectra, variation in the position and intensity of C–Cl peaks supported the existence of hydrogen bonding which rendered Ar /PVC blend miscible.

## Mechanical testing

A relative investigation of mechanical properties of Ar/PVC and PVC/Ar blends was carried out, and the data from mechanical testing of blend systems is given in Tables 1 and 2, respectively.

In one endeavor, dispersion of 0 to 50 wt% PVC in Ar matrix resulted in Ar/PVC blend films which were pinkish in color and color intensified with increasing amount of PVC. The stress–strain isotherms for these blended polymeric materials are given in Fig. 3. Values of the moduli integrated from the stress–strain data displayed that the maximum value of modulus (2,299 MPa) corresponded to 40 wt% PVC contents in the Ar matrix. The maximum stress was found to increase initially with increase in the PVC contents and, at 40 wt% PVC, exhibited a maximum value of 96 MPa relative to the neat Ar (70 MPa) and neat PVC (10 MPa), which is indicative of improvement in tensile strength (Fig. 3). The incorporation of Ar reinforces the PVC matrix, depicting the observed enhancement in the tensile strength compared to neat PVC. Maximum strain for blends increased with PVC contents along with slight

**Table 2** Mechanical data of PVC-Ar blends

| Percent PVC | Maximum stress (MPa) ±0.03 | Maximum strain ±0.03 | Modulus (MPa) ±0.02 | Toughness (MPa) ±0.50 |
|---|---|---|---|---|
| 100 | 10.20 | 2.51 | 531.80 | 22.52 |
| 90 | 22.40 | 1.50 | 1110.15 | 27.95 |
| 80 | 26.91 | 2.84 | 894.02 | 65.88 |
| 70 | 19.38 | 2.84 | 154.84 | 39.47 |
| 60 | 19.38 | 2.84 | 109.48 | 39.56 |
| 50 | 29.12 | 3.33 | 327.89 | 74.28 |
| 0 | 70.37 | 1.00 | 2288.97 | 62.00 |

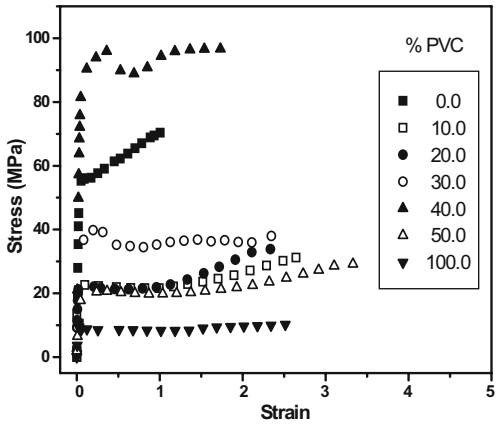


**Fig. 3** Stress–strain curves of Ar/PVC blends

variation in the results (Table 1). The mechanical profile demonstrated an increase in tensile properties up to 40wt% PVC, followed by a gradual decrease. The improvement in the mechanical properties is presumably from the compatibility between polyamide matrix and PVC chains. The mechanical profile of the various blends illustrated that the miscibility of two polymers was maximum when Ar and PVC were mixed in 60:40 ratio because the blend of this composition demonstrated enhancement in the mechanical properties, i.e., the stress, toughness, and modulus values of the blend were optimum vs rest of the Ar/PVC blend compositions. Maximum interaction between Ar and PVC can be achieved when PVC chains are fully dispersed homogenously throughout the matrix. In this case, the optimal concentration of PVC was 40wt % in the Ar matrix. The improvements in the tensile properties of the blends are accredited to the intermolecular forces. Hydrogen bonding is believed to enhance the mechanical properties of two polymers by operating between the hydrogen atom of PVC chains and carbonyl group of polyamide, thus rendering the miscibility of two matrices. The presence of hydrogen bonding also dispenses negative free energy of mixing thus facilitating miscibility, hence, engendering better mechanical properties (Fig. 4).

For PVC/Ar system, blends were prepared by variations in the concentration of PVC from 50 to 100wt% PVC, and films thus obtained were subjected to tensile measurements.

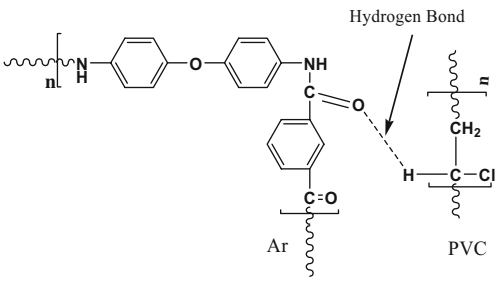


**Fig. 4** Schematic representation of interaction in Ar/PVC blends

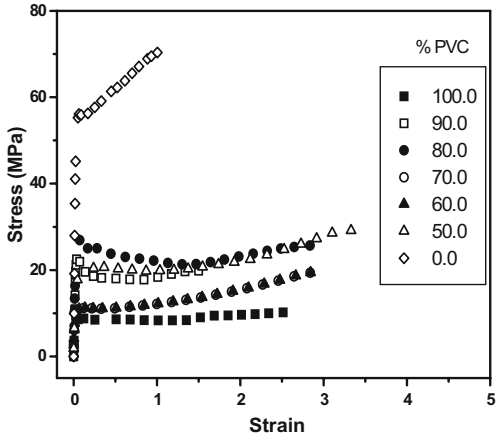


**Fig. 5** Stress–strain curves of PVC/Ar blends

Variations in tensile strength of PVC/Ar blends with increase in Ar contents are illustrated in Fig. 5 and Table 2. Tensile modulus demonstrated initial increase and subsequent decrease with the addition of Ar to PVC (Fig. 5). The stress increased up to 26.91 MPa for 80wt% PVC and then gradually decreased with decrease in the addition of PVC (Table 2). The stress values observed in all PVC/Ar blend samples were greater than neat PVC but smaller than virgin Ar. Fig. 5 displays an increase in the length at rupture of blends relative to both neat Ar and PVC. Table 2 depicts the variation of the toughness as a function of PVC in Ar. Up to 80 wt% of PVC addition, the regularly arranged polyamide chains were distributed irregularly, and so, the entropy of system increased and resulted in the stable blends. Below 80 wt% PVC, further increase in the entropy was not possible, and so, the miscibility decreased, and phase separation occurred, which resulted in the decrease of the mechanical properties.

In essence, toughness and mechanical properties of the Ar/PVC system have improved significantly compared to the PVC/Ar system. This trend may be explained in terms of the plasticization effect. PVC/Ar blends displayed a significant reduction in mechanical profile owing to the inefficient stress transfer across the interface.

## Microscopy

The shape and homogeneity of dispersed phase was analyzed by SEM of cryo-fractured surfaces. Fig. 6a–d demonstrates the micrographs of fractured surfaces from 30 to 40 wt% Ar/PVC blends possessing optimum thermal and mechanical traits. Microscopic results are in good compliance with the thermogravimetric studies. The drastic reduction in $T_g$ of Ar/PVC blends is suggestive of single-phase morphology. Owing to the specific interactions in Ar/PVC blends, sufficient compatibilization is allowed to engender small-phase domains (Fig. 6), whereas improved morphological properties are characteristic of good interfacial cohesion through specific interactions. In this case, H-bonding operates between blend components to diminish phase size thus rendering miscibility. Validation of this assumption is rationalized through the presence of specific interactions (H-bonding) between matrices (Fig. 4) which proves useful in predicting stability. A strong correlation between thermal and morphological behaviors is accredited

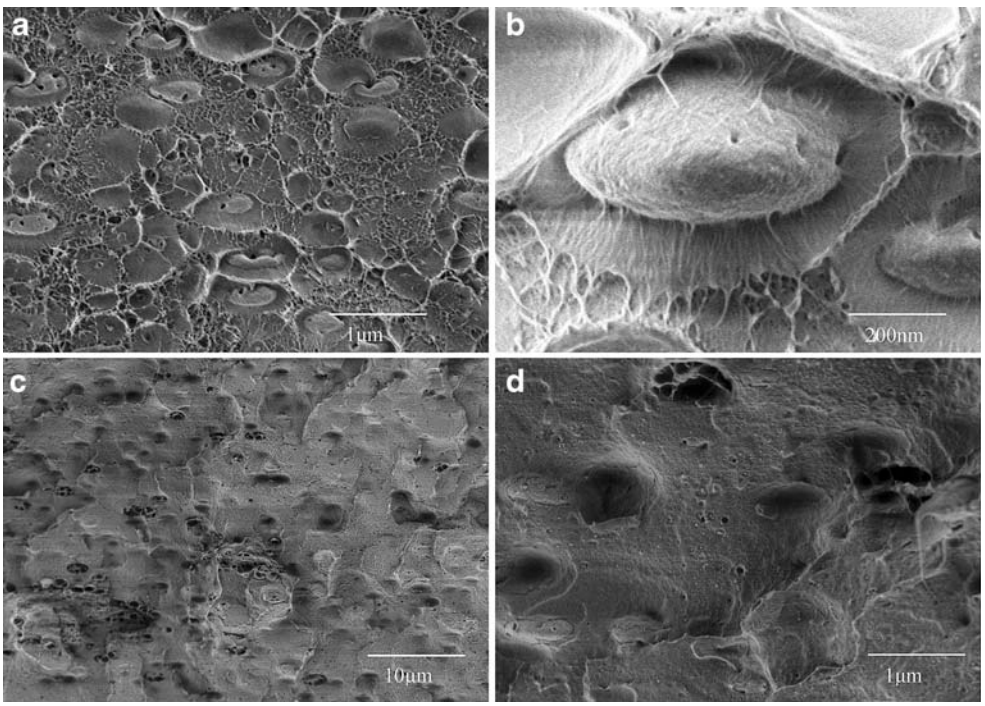


**Fig. 6** SEM micrographs of Ar/PVC blends: **a**–**b** 30 wt% PVC; **c**–**d** 40 wt% PVC

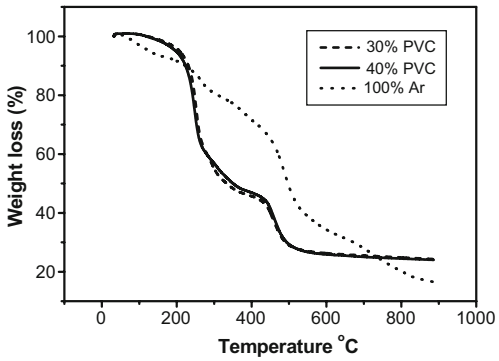


**Fig. 7** Thermogravimetric curves of pure Ar, 30 and 40 wt% Ar/PVC blends

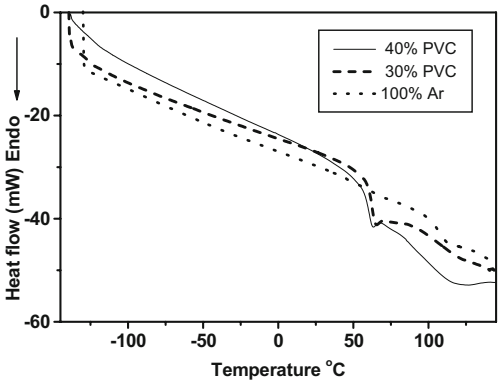


**Fig. 8** DSC curves of pure Ar, 30 and 40 wt% Ar/PVC blends

to the profound effect of a stabilized morphology; further reinforced by the enhanced mechanical properties of the compositions under consideration. A uniform dispersion of blend constituents is revealed from the appearance of morphology exhibited in micrographs, and the continuous phase morphology (Fig. 6) is an evidence for a good interfacial cohesion. These results are also in conformity with the mechanical property profile. In short, a uniform and stable morphology is traced by virtue of strong interactions between the matrix and dispersed phases, which tend to promote miscibility resulting in enhancement of thermal and mechanical facades.

## Thermal stability

In assessing the miscibility effect on the thermal properties, percent weight loss and $T_g$ values were selected as representative traits. The thermal degradation temperatures of PVC/Ar blends were determined using thermogravimetric analysis. From the TG curves of 30 to 40 wt% PVC blends presented in Fig. 7, weight losses at different temperatures and the temperature at maximum rate of degradation ($T_{max}$) were determined. Table 3 gives the percent weight loss of the specimen that remained at four selected temperatures viz, 400, 420, 440, and 460°C. In both blend samples, a gradual increase in weight loss can be noticed (at 400 and 420°C) indicating their thermal stability, whereas, at 440 and 460°C an appreciable change in weight loss was observed. But it should be emphasized that the weight loss at all selected temperatures for both blends was comparable. The temperature at maximum rate of degradation ($T_{max}$) has been employed to evaluate the relative thermal stability of blends. The $T_{max}$ was found to be 783 K for 40 wt% PVC blend, which is even higher than the corresponding 30 wt% PVC blend (776 K); so, as the concentration of the PVC phase in the blend decreases, the thermal stability of the blend also decreases. From Table 3, it can be seen that both blend compositions exhibit one $T_{max}$ corresponding to the degradation, which is a direct indication of high miscibility and compatibility of the PVC Ar blends. Subsequently, the additional evidence for the mutual stability of Ar/PVC blends is available from the DSC thermograms shown in Fig. 8. Glass transition temperature of 100 wt% PVC is 74°C as reported earlier [35]. For both compositions, blends exhibit only a single $T_g$ corresponding to the cooperative segmental motion of the molecular chains. This recommended single phase morphology in these PVC/Ar blends. Blends exhibit a shift to higher $T_g$ value as PVC content increases. It is quite evident from solitary $T_g$ value of blends, intermediate between the $T_g$ of individual components, that the blend systems are compatible (Table 4). In brief, electrostatic interactions have been considered to explain the miscibility in polymer blends. In miscible blends involving PVC, chlorine atoms of PVC interact with atoms of another polymer, having nonbonded electrons, like oxygen, nitro-

**Table 3** Effect of blend ratio on $T_{max}$ and weight losses at different temperatures

| Blend | Weight loss at temperature (%) | | | | $T_{max}$ (K) |
|---|---|---|---|---|---|
| | 400°C | 420°C | 440°C | 460°C | |
| 30 wt% PVC | 54.35 | 55.46 | 57.63 | 63.07 | 776 |
| 40 wt% PVC | 53.11 | 54.23 | 56.21 | 61.70 | 783 |

**Table 4** $T_g$ values of virgin PVC and aramid matrices versus blend compositions

| System | $T_g$ (°C) |
|---|---|
| 100 wt% PVC | 74.00* |
| 100 wt% Ar | 105.10 |
| 30 wt% Ar/PVC blend | 53.88 |
| 40-wt. % Ar/PVC blend | 55.74 |

Bibi et al. 2007 [35]

gen, or others [31–33]. Accordingly, the miscibility of the PVC/Ar blends could be explained in terms of donor–acceptor interactions between chlorine atoms (weak acceptor species) and oxygen atoms (donor species) of the Ar chains. Furthermore, the hydrogen bond operating between the hydrogen atoms of PVC and carbonyl groups of aromatic polyamide is also responsible for the miscibility of two matrices.

As seen from Fig. 7, TGA curve of the 100-wt% Ar shows one step which is attributed to the aromatic polyamide degradation. Thermograms for both 30 and 40 wt% PVC compositions are presented in Fig. 7, respectively. The organic matter started to decompose in the Ar/PVC blend near 235°C. The first step is the dehydrochlorination of the organic polymer chains resulting in the formation of polyene sequences of different lengths [34]. PVC generally shows two stages of decomposition: during the first stage (between 200 and 360°C), it is mainly HCl, benzene, and very small amounts of alkyl aromatic or condensed ring aromatic hydrocarbons that are formed. Nearly, 15% of the polyene generates benzene, the main part accumulating in the polymer and being active in intermolecular condensation reactions, by which cyclohexane and cyclohexadiene rings embedded in an aliphatic matrix are formed [35].

Alkyl aromatics and condensed ring aromatic hydrocarbons are created in the second stage of degradation between 360 and 500°C. In this stage, the polymeric network formed by polyene condensation breaks down in the process of aromatization of the above six carbon rings. The thermal decomposition temperature of the pure PVC lies between 230 and 255°C [35]. For the system under study, the $T_{max}$ of Ar/PVC blends rises; thus, the thermal stability of the material is improved. The interaction between Ar and PVC matrices serves to enhance thermal properties. However, only an appropriate amount of the two phases provided better compatibility, which in case of Ar/PVC blends was up to 40 wt% PVC.

There are stronger interactions between blend components; this is attributed to the polar groups in the polymer chains, e.g., C=O groups distributed in the Ar matrix which can form secondary bonds with the hydrogen atoms of PVC. As the interaction between the two constituents has a profound effect on the properties of the resulting blends, thus, the increment in the property profile of the blends confirm the complete miscibility of the matrices [35]. Miscibility has been achieved by virtue of the greater interfacial bonding between the two phases. Consequently, Ar promotes processability of PVC and reduces the internal friction of the PVC molecules thereby reducing the $T_g$ value. The reduction in $T_g$ of Ar/PVC blends advocates the greater low temperature flexibility thus making processability easy.

## Conclusions

It has been verified that there is an essential correlation between thermal, mechanical, and morphological properties. The glass transition temperatures obtained from DSC thermograms exhibit a single $T_g$ lying between the $T_g$s of the blend components, thus, indicating miscibility. Stable phase morphology has been established by morphological results; which is ascribed to the interfacial adhesion through H-bonding between matrices. PVC, 40 wt%, blend exhibits better synergy, as reflected by improved mechanical properties. The system under study has revealed specific interactions so as to reduce the dispersed phase size. As a consequence, the diminution in $T_g$ of Ar/PVC blends conspicuously validates the augmentation of PVC processability without deteriorating mechanical persona.

**Acknowledgements** Special thanks are due to Dr. Gerhard Wegner, Director, MPI-P for providing the characterization facilities for the completion of this work.

## References

1. Ovchinnikov YV, Tetel, Baum BY, Maklakov AJ (1971) Vysokomol Soedin Ser A 13:2422
2. Olabisi O (1975) Macromolecules 8:316
3. Benedetti E, Posar F, D'alessio A, Vergdmini P, Ciardelli F (1985) J Polym Sci, Polym Phys Ed 23:1187
4. Benedetti E, D'alessio A, Aglietto M, Ruggeri G, Vergdmini P, Ciardelli F (1986) Polym Eng Sci 26:9
5. Varughese KT, Nando GB, De PP, De SK (1988) J Mater Sci 23:3894
6. Margaritis AG, Kalfoglou NK (1987) Polymer 28:497
7. Varughese KT, Sanyal SK (1989) J Appl Polym Sci 37:2537
8. Akiba I, Ohba Y, Akiyama S (1999) Macromolecules 32:1175
9. Varghese H, Bhagavan SS, Thomas S (2001) J Therm Anal Calorim 63:749
10. Varghese H, Johnson T, Bhagavan SS, Joseph S, Thomas S, Groeninckx G (2002) J Polym Sci B Polym Phys 40:1556
11. Stack S, O'Donogbue O, Birkinshaw C (2003) Polym Degrad Stab 79:29
12. Vrandecic´ NS, Klaric´ I, Kovacic´ T (2004) Polym Degrad Stab 84:23
13. Santra RN, Mukundo PG, Chaki TK, Nando GB (1993) Thermochim Acta 219:283
14. Lizymol PP, Thomas S (1993) Polym Degrad Stab 41:59
15. Asaletha R, Kumaran MG, Thomas S (1998) Polym Degrad Stab 61:431
16. Oommen Z, Groeninckx G, Thomas S (2000) J Polym Sci B Polym Phys 38:525
17. Neiro SMS, Dragunski DC, Rubira AF, Muniz EC (2000) Eur Polym J 36:583
18. Kato T (2000) Struct Bond 96:95
19. Song M, Long F (1991) Eur Polym J 27:983
20. Lavallee C, Carmel M, Utracki LA, Szabo JP, Keough IA, Favis BD (1992) Polym Eng Sci 32:1716
21. Bekturov EA, Bimendia LA (1982) Adv Polym Sci 41:99
22. Moskala EJ, Varnell DF, Coleman MM (1985) Polymer 26:228

23. Wang LF, Pearce EM, Kwei TK (1991) J Polym Sci Polym Phys Ed 29:619
24. Hjertberg T, Sorvic EM (1983) Polymer 24:685
25. Talamini G, Pezzin G (1960) Makromol Chem 39:26
26. Avaldi AC (1964) J Appl Polym Sci 8:747
27. Pezzin G (1967) J Appl Polym Sci 11:2553
28. Kim BK, Shin GS, Kim YJ, Park TS (1993) J Appl Sci 47:1581
29. Pecora R, Berne J (1976) Dynamic Light Scattering. Plenum, New York
30. Chu B (1991) Laser Light Scattering. Academic, New York
31. Olabisi O, Robeson LM, Shaw MT (1979) Polymer–Polymer Miscibility. Academic, New York
32. Marco C, Gomez MA, Fatou JG, Etxeberria A, Elorza MM, Irvin JJ (1993) Eur Polym J 29:1477
33. Ramesh S, Yahaya AH, Arof AK (2002) Solid State Ionics 148:483
34. Ivan B, Kelen T, Tudos F (1989) Degradation and stabilization of polymers. Elsevier, New York
35. Bibi N, Sarwar MI, Ishaq M, Ahmad Z (2007) Polymers and Polymer Composites 15:313